




## Research Article

# Tilapia Skin Peptides Inhibit Apoptosis, Inflammation, and Oxidative Stress to Improve Dry Eye Disease *In Vitro* and *In Vivo*

Jian Zeng <sup>1</sup>, Chuanyin Hu <sup>2</sup>, Cuixian Lin,<sup>1</sup> Shilin Zhang,<sup>1</sup> Kaishu Deng,<sup>1</sup> Jianyang Du,<sup>3</sup> Zhiyou Yang,<sup>1</sup> Shucheng Liu,<sup>1</sup> Wenjin Wu,<sup>4</sup> and Yun-Tao Zhao <sup>1</sup>

<sup>1</sup>College of Food Science and Technology, Modern Biochemistry Experimental Center, Guangdong Ocean University, Guangdong Province Engineering Laboratory for Marine Biological Products, Guangdong Provincial Key Laboratory of Aquatic Product Processing and Safety, Zhanjiang 524088, China

<sup>2</sup>Department of Biology, Guangdong Medical University, Zhanjiang 524023, China

<sup>3</sup>Department of Anatomy and Neurobiology, University of Tennessee Health Science Center, Memphis, TN 38163, USA

<sup>4</sup>Institute of Agricultural Products Processing and Nuclear Agricultural Technology, Hubei Academy of Agricultural Sciences, Wuhan 430064, China

Correspondence should be addressed to Yun-Tao Zhao; zhaoyt@gdou.edu.cn

Received 11 February 2023; Revised 4 June 2023; Accepted 15 June 2023; Published 22 June 2023

Academic Editor: Miguel Rebollo-Hernanz

Copyright © 2023 Jian Zeng et al. This is an open access article distributed under the Creative Commons Attribution License, which permits unrestricted use, distribution, and reproduction in any medium, provided the original work is properly cited.

Dry eye disease (DED) is a common chronic ophthalmic disorder, and there is no effective treatment to cure it. It is urgent to find new antidry eye compounds. Here, the effects and underlying mechanisms of tilapia skin peptides (TSP) on DED were investigated. *In vitro*, human corneal epithelial cells (HCECs) were cultured in a hypertonic medium containing TSP for 12 h. The MTT assay, calcein-AM/PI staining, reactive oxygen (ROS) analysis, and western blot were performed at the end of the experiments. In the *in vivo* model of DED, mice eyes were dropped with 0.3% benzalkonium chloride (BAC) and 0.1% TSP for 14 days. Mice were treated with BAC and TSP twice daily with a 10-hour time interval between treatments. After treatment, phenolic red cotton experiment, tear ferning test, and histology assay were carried out. *In vitro*, TSP significantly restored the cell viability of HCECs challenged by NaCl. *In vivo*, tear secretion function and tear fern-like crystal levels were considerably improved in the DED group after treatment with TSP. Mechanically, TSP impend the DED development by regulating Bax/Bcl-2 signal pathway, inhibiting iNOS and COX-2 protein expression, moderating ROS/Nrf2/HO-1 axis, inhibiting cell apoptosis in the corneal regions, increasing the number of conjunctival goblet cells, and arresting corneal epithelial thinning. In conclusion, TSP ameliorated DED-like disorder in BAC-induced DED mice and cell damage in NaCl-induced HCECs. TSP improved DED by suppressing apoptosis, inflammation, and oxidative stress. Consequently, this study reveals the beneficial activity of TSP in DED.

## 1. Introduction

Dry eye disease (DED), one of the most common chronic diseases in ophthalmic clinics, distresses 5% to 50% of people around the world [1, 2]. Increasing epidemiological evidence indicates that DED is more prevalent in women than in men. As population ages, the incidence of DED is increasing annually [3, 4]. Previous studies have shown that DED is related to lifestyle habits, such as smoking, drinking alcohol, using electronic screens, and wearing contact lenses for

a long time [5, 6]. In addition, certain autologous diseases, air pollution, lack of sleep, and dry environments increase the risk of suffering from DED [7–9]. DED causes ocular pain or discomfort, and even worse, severe DED affects the patient's vision and mental health [10, 11].

Conventional therapy for DED mainly depends on artificial tears intervention to enhance lubrication on ocular surface and improve eye inflammation [12]. However, there are some drawbacks after treatment with artificial tears. For example, cyclosporine A, a drug commonly used to treat

DED, causes undesirable effects such as ocular surface pain, burning sensations, bone marrow suppression, cystitis, and hypertension [13]. Studies point out that prolonged use of corticosteroids for the treatment of DED increases the risk of hypertension, glaucoma, and cataracts [14]. To date, the effectiveness of the treatment for DED is suboptimal, and effective drugs for DED remain a major unmet need.

China produces more than 90% of the world's tilapia and holds the world's largest production of freshwater fish [15]. Unfortunately, many by-products, including skin, are generated because tilapia is often only processed into primary products such as fillets [16]. Most of those by-products are discarded as rubbish, which contributes to environmental pollution and wastage of resources. Sourcing active substances from tilapia skin would not only help alleviate the problem of wasted resources and environmental pollution but also promote the upgradation of the tilapia industry [17]. In addition, studies have shown that natural foods and nutritional support provide a valuable intervention in the prevention and treatment of ocular diseases [18]. Tilapia skin peptides (TSP) are prepared enzymatically from tilapia skin and characterized by good biocompatibility, high solubility, safety, nontoxicity, and easy digestion and absorption [19]. Several biological activities of TSP, such as promotion of wound healing, antioxidant, improvement of diabetes, antihypertensive, and antidepressant, have been reported in previous studies [20–24]. To date, the role of TSP on DED has not been reported.

Here, the effects of TSP on DED were explored. Meanwhile, the relevant mechanisms of TSP on DED were investigated *via in vitro* and *in vivo* DED models.

## 2. Materials and Methods

**2.1. Materials.** Human corneal epithelial cells (HCECs) were purchased from Guangzhou Jennio Biotech Co., Ltd (Guangzhou, China). Sodium hyaluronate (SH, H20150150) eye drops were obtained from URSAPHARM Arzneimittel GmbH (Saarbrücken, Germany). Benzalkonium chloride (BAC, C12506740) was bought from Shanghai Macklin Biochemical Technology Co., Ltd (Shanghai, China). Tear test phenol red cotton thread was acquired from Tianjin Jingming New Technological Development Co., Ltd (Tianjin, China). The *in situ* terminal deoxynucleotidyl transferase-mediated dUTP biotin nick end labeling kit (TUNEL, E-CK-A321) was obtained from Elabscience Biotechnology Co., Ltd (Wuhan, China). The 3-(4,5)-dimethylthiazoliazolo(-z-y1)-3,5-diphenyltetrazolium bromide (MTT, S19063) was obtained from Shanghai Yuanye Biotechnology Co., Ltd (Shanghai, China). Radioimmunoprecipitation assay buffer (RIPA buffer, P0013B), periodic acid-Schiff (PAS, C0142S) staining Kit, hematoxylin and eosin (H&E, C0105S) staining kit, BCA Protein Quantification Kit (P0012), and calcein cetoxy methylester kit (calcein-AM, C2013FT) were obtained from Beyotime Biotechnology Co., Ltd (Shanghai, China). Propidium iodide (PI, 81845) was sourced from Sigma-Aldrich (St. Louis, MO, USA). The 2,7-dichlorodihydrofluorescein diacetate (DCFH-DA, C2938) was taken from molecular probes

(Carlsbad, CA, USA). The anti-B-cell lymphoma-2 (Bcl-2, SC-7382) and anti-Bcl-2-associated X (Bax, SC-7480) antibodies were obtained from Santa Cruz (Dallas, TX, USA). The antiheme oxygenase-1 (HO-1, ab68477) antibody was bought from Abcam (Cambridge, UK). The antinuclear factor E2-related factor (Nrf2, 20733), anticyclooxygenase 2 (COX-2, 12282S), and anti- $\beta$ -actin (4970) antibody were obtained from Cell Signal Technology (Danvers, MA, USA). The antiinducible nitric oxide synthase (iNOS, WL0992a) antibody was obtained from Wanleibio CO., Ltd (Shenyang, China). The polyvinylidene difluoride (PVDF) membranes were obtained from Merck Millipore (IPVH00010, Millipore, MA, USA). Modified eagle's medium (MEM, 11095080), fetal bovine serum (FBS, 1907422), and penicillin-streptomycin solution (2289325) were obtained from Gibco (Grand Island, USA).

**2.2. Preparation of TSP.** The preparation method of TSP was described in our previous article [25]. Briefly, tilapia skins were defatted with isopropyl alcohol and then dried. Dried skins were first hydrolyzed by 0.3% neutrase for 90 min at 50°C, pH 7.0, followed by 0.3% alcalase for 90 min at 55°C, pH 9.0, respectively. The hydrolysis solution was heated (90°C for 10 mins) and centrifuged (12000g for 15 mins). The supernatant was ultrafiltered with a 10 kDa ultrafiltration membrane and then freeze-dried to obtain the dry powder, which was named TSP. Glycine was the most abundant amino acid in TSP prepared according to this method, followed by proline, arginine, and alanine [25]. Most of TSP were small molecular peptides with molecular weight less than 3 kDa (92.63%) [25].

**2.3. Cell Culture and Treatment.** HCECs were grown in MEM medium containing 10% FBS, 100  $\mu$ g/mL streptomycin, and 100 U/mL penicillin. HCECs were cultured in a cell incubator under 5% CO<sub>2</sub> at 37°C.

HCEC viabilities were detected by the MTT method.  $2 \times 10^4$  cells/well were plated into 96-well plates to be pro-cultured for 24 h. To find the appropriate modeling concentration, HCECs were incubated with different concentrations of NaCl (0 mM, 20 mM, 40 mM, 60 mM, 80 mM, and 100 mM, respectively) for 12 h. For testing cytotoxicity, the individual concentrations of TSP (0  $\mu$ g/mL, 250  $\mu$ g/mL, 500  $\mu$ g/mL, 1000  $\mu$ g/mL, and 2000  $\mu$ g/mL, respectively) were added to each well and incubated for 12 h. For detecting the protective effects of TSP, HCECs were randomly grouped into 4 groups as follows: control, M (100 mM NaCl), M + TSP (250  $\mu$ g/mL), and M + TSP (500  $\mu$ g/mL). HCECs were pretreated with TSP (250  $\mu$ g/mL or 500  $\mu$ g/mL) for 2 h, and then the cells were co-incubated with 100 mM NaCl and different concentrations of TSP for 12 h. After that, the medium was discarded and cells were washed 3 times with PBS (phosphate buffer solution, pH 7.2). Afterward, 100  $\mu$ L MTT solution (0.5 mg/mL) was added to each well and the cells were incubated for 4 h at 37°C. Finally, the MTT solution was discarded, and 150  $\mu$ L dimethyl sulfoxide was added to dissolve formazan. The

results of the MTT assay were obtained by measuring absorbance at 490 nm *via* a microplate reader (BioTek, USA).

**2.4. Animals and Treatment.** Mice (C57BL/6, male, 6~7 weeks old) were obtained from Guangdong Medical Laboratory Animal Center (Guangzhou, China). Mice were housed in a standard animal room (room temperature:  $23 \pm 2^\circ\text{C}$ , relative humidity: 40~60%, and light-dark cycled for 12 hours from 8:00 a.m. to 8:00 p.m.). During the experiment period, the mice were not restricted to water and diet. The protocol of animal experiments was approved by the Animal Ethics Committee of Guangdong Ocean University (approval number: 2022062101) and carried out under the requirements of the Guidelines for the Care and Use of Laboratory Animals of Guangdong Ocean University.

The BAC-induced DED mouse model was established according to a previously reported method with minor modifications [26]. The mice were randomly grouped into 4 groups (9 mice per group,  $n = 18$  eyes) as follows: control, DED, DED + TSP, and DED + SH, respectively. SH (sodium hyaluronate) eye drops was used as a positive medicine. After 7 days of acclimatization, mice eyes in the control group were dropped with normal saline ( $5 \mu\text{L}/\text{eye}$ ). Mice eyes in remaining 3 groups were dropped with  $5 \mu\text{L}$  0.3% BAC (dissolved in normal saline). One hour later, each eye in the control and DED groups was dropped with  $5 \mu\text{L}$  normal saline. Each eye in DED + TSP and DED + SH groups was treated by  $5 \mu\text{L}$  0.1% TSP (dissolved in normal saline) or SH, respectively. Eyes treated with different eye drops were started at 8:30 a.m. and repeated at 6:30 p.m. every day for 14 days. Tear volume measurement and tear ferning test were employed on day 15 and 16, respectively. On day 17, mice were euthanized, and the ocular surface tissue was collected.

**2.5. Tear Volume Measurement.** Tear volume measurement was performed as previously reported methods, with slight modification [27]. Briefly, a cotton thread was placed on the inside of the medial side of the lower conjunctiva's fornix for 30 s (Figure 1(b)) [27]. Then, the reddening length of the thread was measured (Figure 1(c)).

**2.6. Tear Ferning Test.** Tear ferning test was carried out according to the reference with minor modifications [28]. In brief, normal saline ( $3 \mu\text{L}$ ) was dropped into the eyeball to wash the ocular surface, and the wash solution was carefully recollected and spread on a clean glass slide. After drying at room temperature for 2 hours, the tear fern-like formation was photographed with a microscope (Leica, Wetzlar, Germany). All measurements were done in a room at  $25^\circ\text{C}$  and relative humidity of 40–50%.

Tear ferns of tears were quantified according to reference [28]. Tear ferning was classified into grades 0 to 4. Grade 0 contains intact crystals with no spaces or gaps between fern crystals. Fern-like crystals in grade 1 have larger interbranch density, spaces, or gaps than those of grade 0. In grade 2, the branch gaps among fern-like crystalline are significantly

larger than those of grade 1. In grade 3, the density between the crystalline branches increases further, and only a few fern-like crystals can be observed. As for grade 4, there were no completely invisible fern-like crystals that can be found.

**2.7. Histology.** After being anesthetized with pentobarbital sodium, mice were transcranial-perfused with PBS and 4% paraformaldehyde. The intact eye tissue (including cornea, upper and lower eyelids, and conjunctiva) was removed. The tissues were bathed in 4% paraformaldehyde at  $4^\circ\text{C}$  for 24 h, dehydrated in graded sucrose solutions, and embedded in paraffin. Sequential  $4 \mu\text{m}$  thick sections of each sample were used for the experiments described in 2.8 and 2.9.

**2.8. Conjunctival Goblet Cells (GCs) Counts and Corneal Epithelial Thickness Measurement.** GCs were stained with PAS staining kit. GCs in the *superior and inferior conjunctiva* in three slides per eye were numbered using Image pro plus software [29]. Seven eyes were counted for each group. H&E staining was carried out to investigate the thickness and morphological changes of corneal epithelial cells. The central corneal thickness of each eye in three sections was calculated using Image J software [30]. Nine eyes were counted for each group.

**2.9. In Situ TUNEL Staining.** *In situ* TUNEL kit was used to detect apoptotic cells in the corneal epithelium. Experimental protocols were carried out strictly under the working instructions of the kit. One representative image of central corneal was obtained from each section under a fluorescence microscope (Leica, Wetzlar, Germany). The number of TUNEL-positive cells in each eye was counted in three sections [31]. Three eyes were counted for each group. Image J was employed to measure the number of apoptotic cells in corneal epithelium.

**2.10. Calcein-AM/PI Staining.** The effects of TSP on apoptosis of HCECs induced by hyperosmotic stress were further measured by calcein-AM/PI staining. The experiment protocol was designed as in the previous study, with slight modifications [32, 33]. After processing the cells as described in section 2.3, the medium was aspirated and HCECs were washed 2 times with PBS. Whereafter, each well was incubated with  $100 \mu\text{L}$  calcein-AM and PI mix for 30 min at  $37^\circ\text{C}$ . Calcein-AM is hydrolyzed into calcein by the endogenous esterase of living cells, which makes living cells emit strong green fluorescence. Dead cells will fluoresce red because PI will only stain dead cells. The images were photographed *via* a fluorescence microscope (Leica, Wetzlar, Germany). The results of calcein-AM/PI staining were described as the relative apoptosis rate (%) which is expressed as a percentage relative to the M group.

**2.11. Intracellular Reactive Oxygen (ROS) Analysis.** The ROS production level in HCECs was measured as previously reported methods [34]. Briefly, HCECs were seeded into

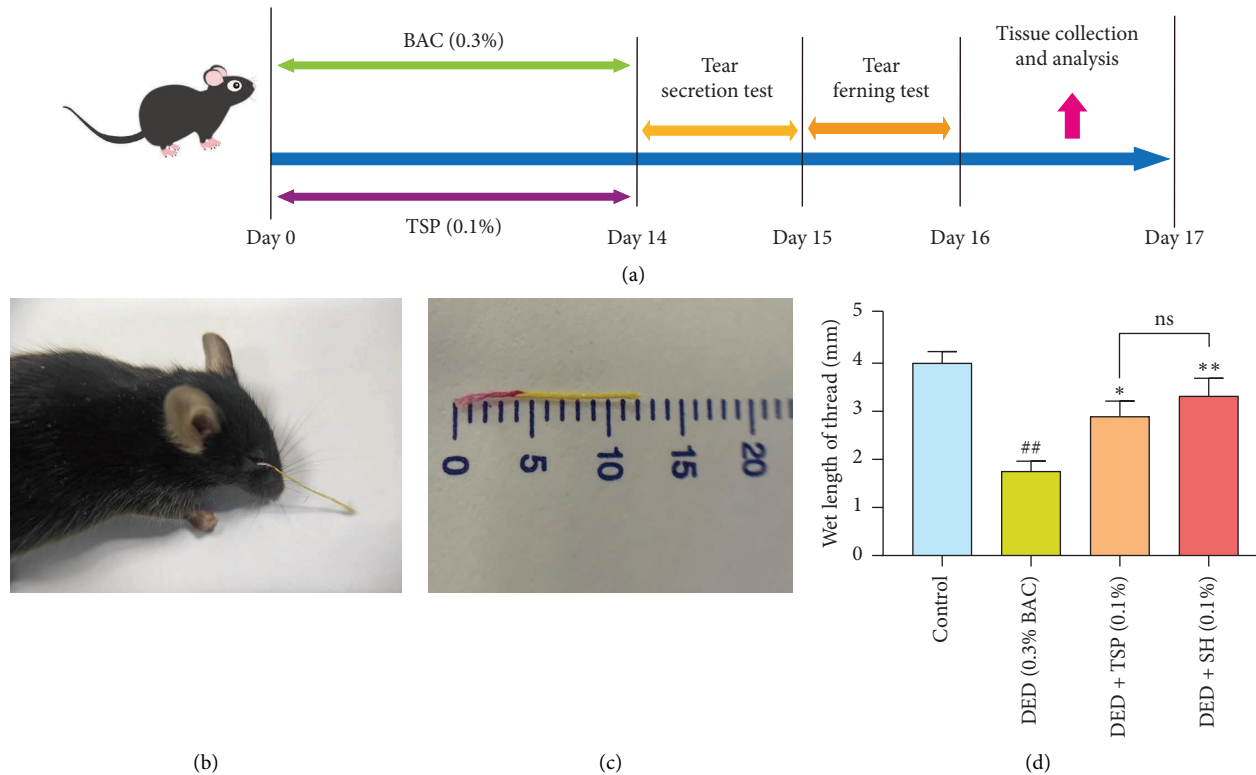


FIGURE 1: Effects of TSP on tear production in benzalkonium chloride (BAC)-induced DED mice. (a) Illustration of the experimental procedure. (b) Schematic diagram of tear secretion test. The cotton thread was placed in the inferior conjunctival fornix for 30 s to test tear production of the mice. (c) Schematic diagram of the length of the cotton reddening. After 30 s, the length of the cotton thread that turned red was calculated with the measuring card. (d) Tear production results ( $n = 16$  eyes). Data shown as mean  $\pm$  SEM. ##  $p < 0.01$  vs. control group; \*  $p < 0.05$ , \*\*  $p < 0.01$  vs. DED group.

black microtiter plates and treated as described in Section 2.2. The medium in each well was aspirated away, and DCFH-DA ( $10 \mu\text{M}$ ) was added to each well for 30 min incubation at  $37^\circ\text{C}$ . The fluorescence image was obtained by a fluorescence microscope (Leica, Wetzlar, Germany). Image J was used to analyze the mean intensity of ROS.

**2.12. Western Blot.** Proteins of HCECs were extracted by RIPA buffer (supplemented with proteinase and phosphatase inhibitors) in an ice bath. During this period, HCECs were placed on a shaker and gently shaken. Then, cells were scraped into one area by cell scrapers, and the lysate was collected. The supernatant was gently gathered after centrifugation at  $12,000 \text{ rpm}$  under  $4^\circ\text{C}$  for 15 min. Following the manufacturer's instructions, the BCA Protein Quantification Kit was used to determine the protein concentration.

Western blot was employed to analyze the protein expression levels of Bcl-2, Bax, COX-2, iNOS, Nrf2, HO-1, and  $\beta$ -actin, and the protocol was designed as our previous method [35]. Mixed proteins from each sample panel were separated by SDS-polyacrylamide gel electrophoresis. Target protein was transferred to PVDF membranes. The membranes were blocked in 5% skim milk powder for 2.5 h at room temperature and then incubated with primary antibodies overnight. Subsequently, the membranes were incubated with horseradish peroxidase-conjugated secondary

antibody for 1 h at room temperature after washing by TBST (Tris Buffered Saline with Tween-20) for 60 min. After washing the membranes with TBST 5 times, the membranes were incubated with an electrochemiluminescence reagent (Millipore, Bedford, MA, USA), and images of the target protein bands were acquired by the ChemiDoc™ XRS+ system (Bio-Rad, Hercules, USA). The density of each band was calculated using Image J. The expression levels of proteins were standardized to  $\beta$ -actin.

**2.13. Statistical Analysis.** Data were analyzed by using Graphpad Prism 8.0. Values are stated as the mean  $\pm$  SEM. One-way ANOVA followed by the Tukey test was used to assess differences between more than three groups. The differences were recognized as significant at  $p < 0.05$ .

### 3. Results

**3.1. TSP Enhanced the Cell Viability of HCECs Challenged by NaCl.** The cytotoxicity of hyperosmotic stress on HCECs is illustrated in Figure 2(a), where NaCl (0 mM, 20 mM, 40 mM, 60 mM, 80 mM, and 100 mM, respectively) decreased the viabilities of HCECs in a concentrate-dependent manner. After being treated with NaCl at the dose of 100 mM, the viability of HCECs was decreased to 70.47% ( $p < 0.01$  vs. control group, Figure 2(a)). Concentration of

100 mM of NaCl was considered as a suitable modeling concentration and used for subsequent experiments. The cytotoxicity data of TSP on HCECs are shown in Figure 2(b). TSP at concentrations with 1000  $\mu\text{g}/\text{mL}$  and 2000  $\mu\text{g}/\text{mL}$  reduced HCECs viabilities to 89.94% ( $p < 0.01$  vs. control group) and 77.08% ( $p < 0.01$  vs. control group), respectively. The results implied that TSP above 1000  $\mu\text{g}/\text{mL}$  produced cytotoxicity to HCECs (Figure 2(b)). The protective effects of TSP on HCECs induced by 100 mM NaCl are displayed in Figure 2(c). In Figure 2(c), the viability of HCECs in the M group is reduced to 67.87% ( $p < 0.01$  vs. control group). After TSP intervention (250  $\mu\text{g}/\text{mL}$  and 500  $\mu\text{g}/\text{mL}$ ), the cell viabilities of HCECs were increased to 81.05% ( $p < 0.01$  vs. M group) and 77.26% ( $p < 0.05$  vs. M group), respectively.

### 3.2. TSP Improved Tear Secretion in BAC-Induced DED Mice.

The experimental protocol for mice is shown in Figure 1(a). All intervention treatments on the mice were completed on day 14. On day 15, phenol red cotton thread experiment was performed to examine the effect of TSP on tear secretion of BAC-induced DED mice (Figures 1(a)–1(c)). The data showed that the reddened length of the cotton thread in the control group was 4.0 mm (Figure 1(d)). In the DED group, the reddened length of the cotton thread was reduced to 1.8 mm, which was significantly shorter than that of the control group ( $p < 0.01$ , Figure 1(d)). The reddening length of the cotton thread in the DED + TSP (2.9 mm,  $p < 0.05$ ) group and DED + SH (positive medicine, 3.3 mm,  $p < 0.01$ ) group was significantly more than that of the DED group (Figure 1(d)). The data showed that there was no clear difference in the efficacy of TSP and SH in improving tear secretion function ( $p > 0.05$ , Figure 1(d)).

### 3.3. TSP Improved Tear Ferning Levels in BAC-Induced DED Mice.

On day 16, tear ferning was tested. Morphologically, the tear fern-like crystals in the control group were intact in shape, while those in the DED group were fragmented (Figure 3(a)). The shape of the tear fern-like crystals was significantly restored after intervention with TSP and SH (Figure 3(a)). Statistically, the tear ferning grade in the control group was 1.1 and in the DED group was 2.9 (Figure 3(b)). The data showed that BAC significantly increased the tear ferning grade in the DED group ( $p < 0.01$  vs. control group, Figure 3(b)). After intervention with TSP and SH, the tear ferning grades were reduced to 2.3 ( $p < 0.05$  vs. DED group) and 2.13 ( $p < 0.01$  vs. DED group), respectively (Figure 3(b)). As for the groups of DED + TSP and DED + SH, there was no obvious difference between them ( $p > 0.05$ , Figure 3(b)). It is suggested that comparable efficacy of TSP and SH in improving tear fern crystallization was founded in this research (Figures 3(a) and 3(b)).

**3.4. TSP Prevented the Corneal Epithelial Cell Layers from Thinning in BAC-Induced DED Mice.** The results of H&E staining are displayed in Figure 4(a). In Figure 4(b), the data showed that the thickness of corneal epithelial cell layers in

the DED group (26.15  $\mu\text{m}$ ,  $p < 0.01$ ) was significantly reduced compared with that of the control group (35.19  $\mu\text{m}$ ). After intervention with TSP or SH, the thickness of corneal epithelial cell layers was increased to 30.92  $\mu\text{m}$  ( $p < 0.05$  vs. DED group) and 32.71  $\mu\text{m}$  ( $p < 0.01$  vs. DED group), respectively (Figure 4(b)). The data showed no statistical difference between the TSP and SH intervention groups ( $p > 0.05$ , Figure 4(b)).

### 3.5. TSP Arrested the Loss of CGs in BAC-Induced DED Mice.

PAS staining was carried out to evaluate the number of GCs in the conjunctiva. The data of PAS staining are shown in Figure 5(a). The number of GCs in conjunctiva in the control group and DED group was 122.5 and 49.75, respectively (Figure 5(b)). The results indicated that BAC stimulation significantly reduced the number of CGs in the DED group ( $p < 0.01$  vs. control group, Figure 5(b)). After intervention with TSP and SH, the number of GCs was 88.17 cells ( $p < 0.05$  vs. DED group) and 95.25 cells ( $p < 0.01$  vs. DED group), respectively (Figure 5(b)). No obvious difference was observed between the groups of DED + TSP with DED + SH ( $p > 0.05$ , Figure 5(b)).

### 3.6. TSP Alleviated Corneal Epithelial Cell Apoptosis Induced by BAC-Induced in DED Mice.

To explore the effects of TSP on corneal epithelial cell apoptosis in DED mice-induced by BAC, TUNEL staining was carried out. The data of TUNEL staining are exhibited in Figure 6(a). The number of TUNEL-positive cells (apoptotic cells) in the corneal epithelial of the DED group (17.67 cells) was clearly higher than that of the control group (2.00 cells) ( $p < 0.01$ , Figure 6(b)). Compared with that of the DED group, the number of TUNEL-positive cells in the DED + TSP group and DED + SH group was increased to 9.01 cells ( $p < 0.05$ ) and 6.03 cells ( $p < 0.05$ ), respectively (Figure 6(b)). There was no clear difference between the groups of DED + TSP and DED + SH ( $p > 0.05$ , Figure 6(b)).

### 3.7. TSP Inhibited Apoptosis in HCECs Challenged by NaCl.

To further investigate the roles of TSP on HCECs apoptosis challenged by NaCl, calcein-AM/PI staining and western blot analysis were carried out. The results of calcein-AM/PI staining are displayed in Figure 7(a). In Figure 7(b), the relative apoptosis rate of HCECs in the M group is significantly higher than that of the control group (7.89%,  $p < 0.01$  vs. M group). After intervention with TSP (250  $\mu\text{g}/\text{mL}$  and 500  $\mu\text{g}/\text{mL}$ ), the relative apoptosis rate was reduced to 36.87% ( $p < 0.01$  vs. M group) and 26.54% ( $p < 0.01$  vs. M group), respectively (Figure 7(b)). Expression levels of Bax and Bcl-2 in HCECs were examined *via* western blot (Figure 7(c)). The ratio of Bax/Bcl-2 expression levels of the M group was significantly increased compared with that of the control group ( $p < 0.01$ , Figure 7(d)). TSP at 250  $\mu\text{g}/\text{mL}$  ( $p < 0.01$  vs. M group) and 500  $\mu\text{g}/\text{mL}$  ( $p = 0.13$  vs. M group) reduced the ratio of Bax/Bcl-2 expression levels in HCECs induced by NaCl, compared with that of the M group (Figure 7(d)).

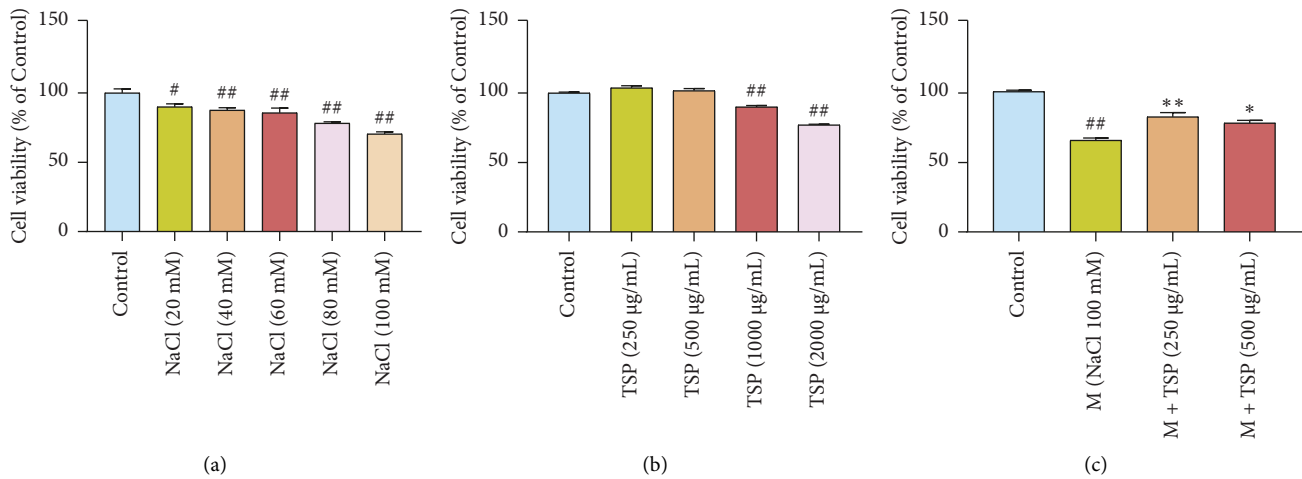


FIGURE 2: Establishment of the dry eye disease (DED) cell model of human corneal epithelial cells (HCECs) and exploration of the effects of tilapia skin peptides (TSP) on the model. (a, b) Effects of different concentrations NaCl (0 mM, 20 mM, 40 mM, 60 mM, 80 mM, and 100 mM, respectively) or TSP (0 µg/mL, 250 µg/mL, 500 µg/mL, 1000 µg/mL, and 2000 µg/mL, respectively) on HCECs. (c) Results of anti-DED activity of TSP *in vitro*. Data are shown as mean  $\pm$  SEM, ( $n = 5$ ); #  $p < 0.05$ , ##  $p < 0.01$  vs. control group; \*  $p < 0.05$ , \*\*  $p < 0.01$  vs. M group.

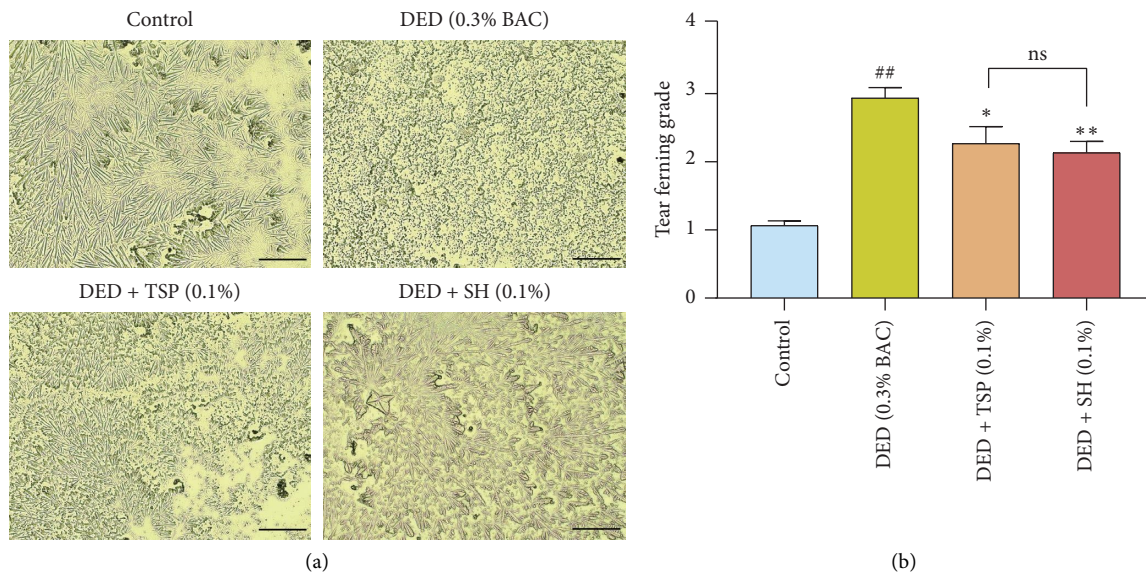


FIGURE 3: Effects of TSP on tear fern in BAC-induced DED mice. (a) Microscopic images of tear fern in BAC-induced DED mice. (scale bar = 50 µm). (b) Results of tear fern grade in BAC-induced DED mice ( $n = 15$  eyes). Data shown as mean  $\pm$  SEM. ##  $p < 0.01$  vs. control group; \*  $p < 0.05$ , \*\*  $p < 0.01$  vs. DED group.

**3.8. TSP Reduced COX-2 and iNOS Protein Expression Level in HCECs Challenged by NaCl.** Expression levels of COX-2 and iNOS in HCECs were assayed (Figures 8(a) and 8(c)). The COX-2 protein expression level in the M group was markedly increased ( $p < 0.01$  vs. control group, Figure 8(b)). After intervention with TSP (250 µg/mL and 500 µg/mL), the expression levels of COX-2 were obviously decreased ( $p < 0.01$  vs. M group, Figure 8(b)). In the M group, the iNOS expression level was higher than that of the control group ( $p < 0.05$ , Figure 8(d)). TSP (250 µg/mL and 500 µg/mL)

treatment significantly downregulated the expression levels of iNOS in HCECs ( $p < 0.05$  vs. M group, Figure 8(d)).

**3.9. TSP Improved ROS/Nrf2/HO-1 Axis in HCECs Challenged by NaCl.** The production level of ROS in the HCECs-challenge by NaCl was detected (Figure 9(a)). The mean intensity of ROS in the M group was markedly increased ( $p < 0.01$  vs. control group Figure 9(b)). After intervention with TSP (250 µg/mL and 500 µg/mL), the mean intensity of

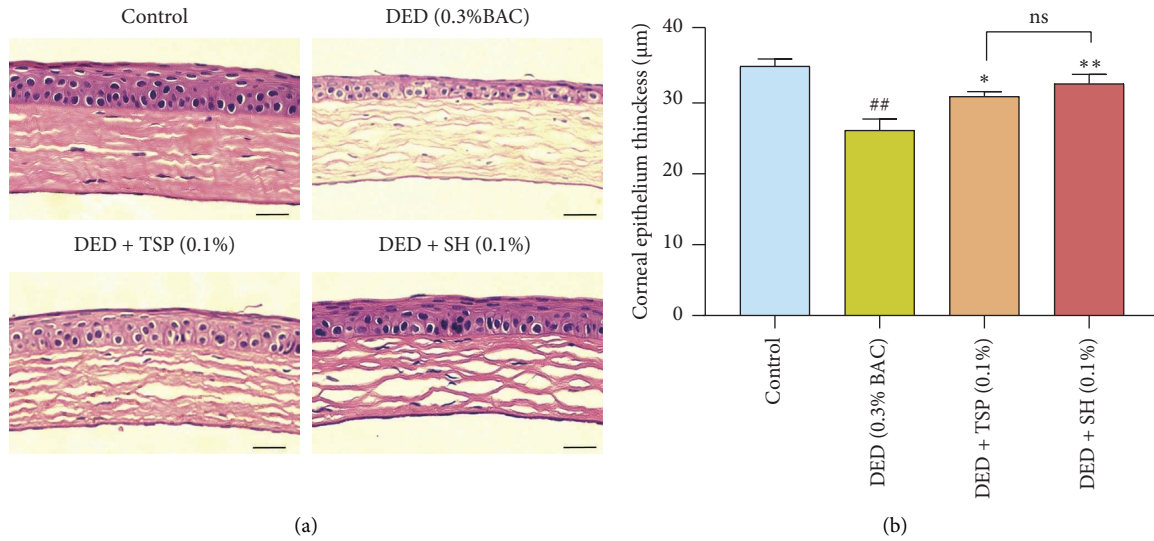


FIGURE 4: Effects of TSP on corneal tissue in BAC-induced DED mice. (a) Microscopic images of H&E staining of corneal tissue in BAC-induced DED mice. (scale bar = 50 μm). (b) Results of changes in the thickness of corneal epithelial cell layers in BAC-induced DED mice ( $n = 9$  eyes). Data shown as mean  $\pm$  SEM. ##  $p < 0.01$  vs. control group; \*  $p < 0.05$ , \*\*  $p < 0.01$  vs. DED group.

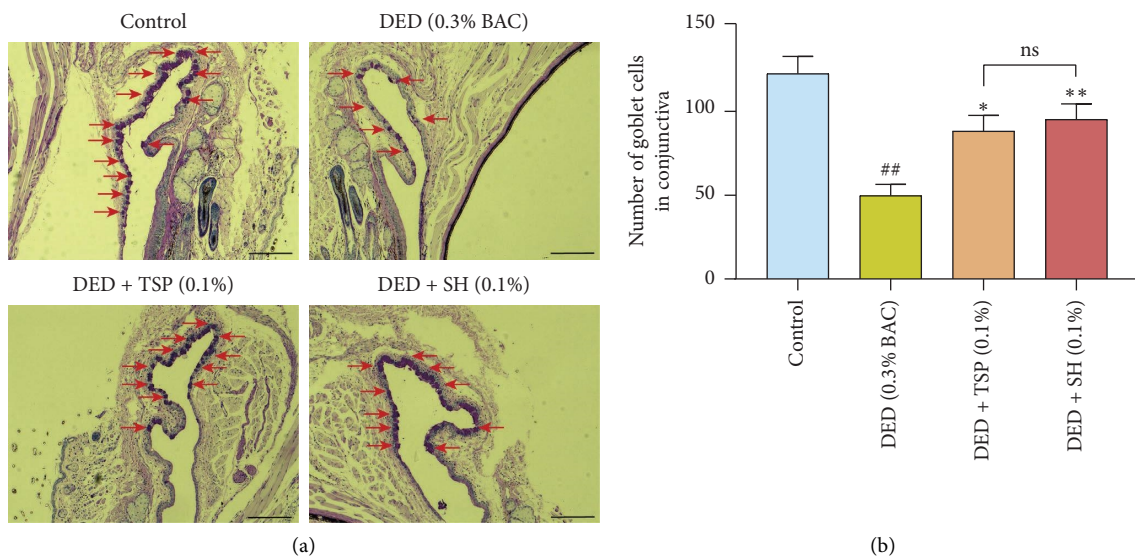


FIGURE 5: Effects of TSP on conjunctival goblet cells (GCs) in BAC-induced DED mice. (a) Microscopic images of PAS staining of corneal tissue in BAC-induced DED mice (scale bar = 50 μm). The red arrows indicate the goblet cells. (b) Results of GC count in BAC-induced DED mice ( $n = 7$  eyes). Data shown as mean  $\pm$  SEM. ##  $p < 0.01$  vs. control group; \*  $p < 0.05$ , \*\*  $p < 0.01$  vs. DED group.

ROS was significantly decreased ( $p < 0.01$  vs. M group;  $p < 0.05$  vs. M group, Figure 9(b)). Expression levels of Nrf2 and HO-1 were obviously downregulated in the M group (both  $p < 0.01$  vs. control group, Figures 9(c)–9(e)). After intervention with TSP (250 μg/mL and 500 μg/mL), the expression levels of Nrf2 were markedly increased ( $p < 0.01$  vs. M group;  $p < 0.05$  vs. M group, Figures 9(c) and 9(d)). TSP (250 μg/mL and 500 μg/mL) intervention also obviously upregulated the expression level of HO-1 in HCECs (both  $p < 0.01$  vs M group, Figures 9(c) and 9(e)).

#### 4. Discussion

DED impairs physical and psychological health of the sufferer. Evidences accumulated over the past few decades indicate that nutritional supplementation helps to prevent DED [36, 37]. As a natural food-derived peptide, TSP is of great benefit to human health. Here, we explored the potential function and mechanisms of TSP on DED in *in vitro* and *in vivo* DED models. NaCl stimulation decreased the cell viability of HCECs, and BAC induction significantly

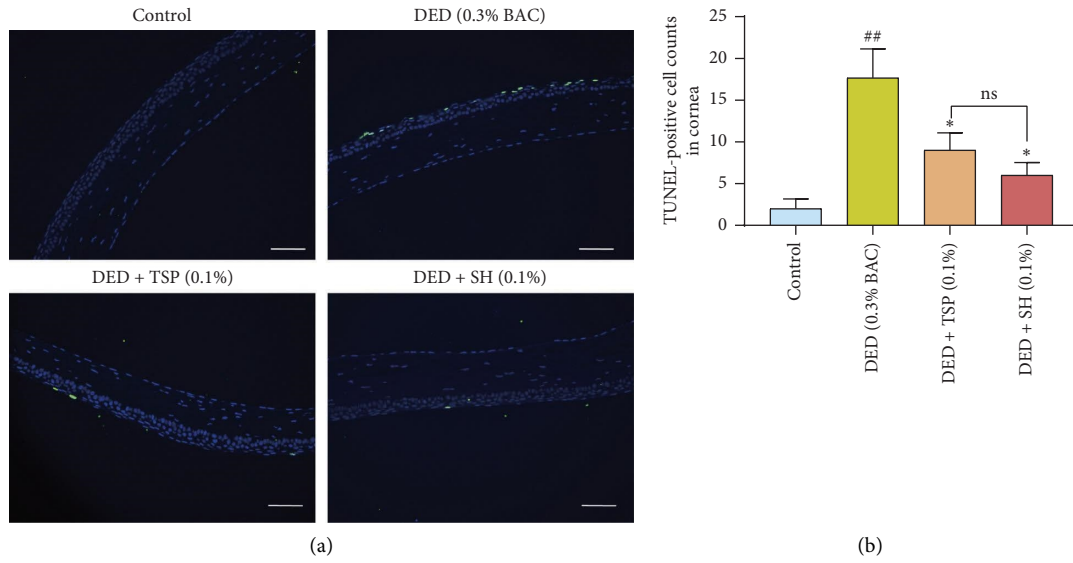


FIGURE 6: Effects of TSP on apoptosis of corneal epithelial cells in DED mice. (a) TUNEL representative picture of corneal epithelial cells apoptosis in BAC-induced DED mice. TUNEL-positive cells, green; DAPI-positive cells, blue. Scale bar = 50 μm. (b) Results of TUNEL-positive cell count in the cornea ( $n = 3$  eyes). Data shown as mean ± SEM. <sup>##</sup> $p < 0.01$  vs. control group; <sup>\*</sup> $p < 0.05$  vs. DED group.

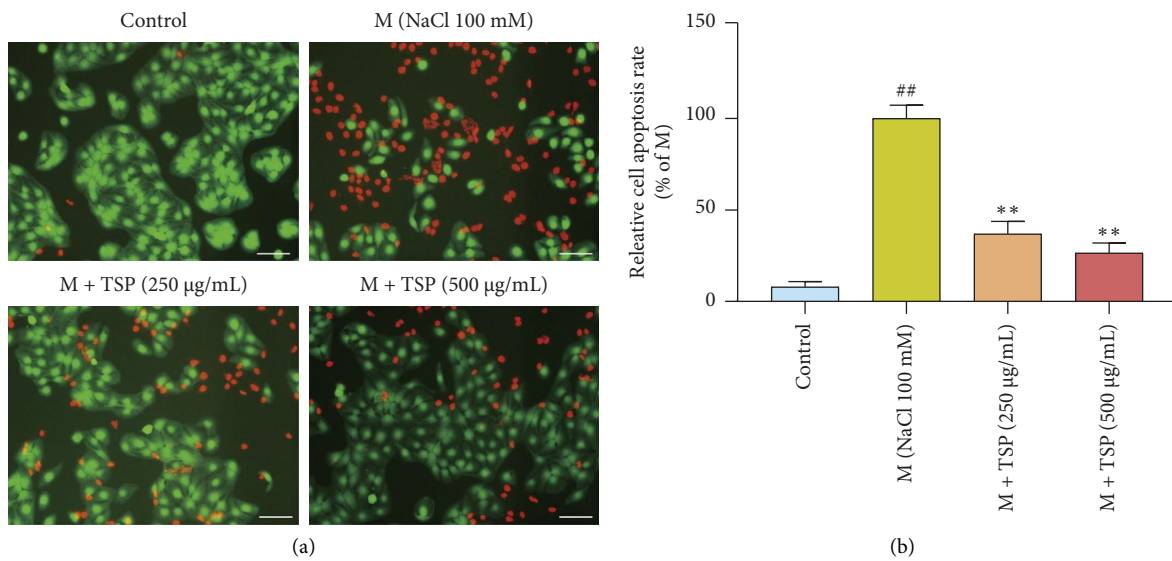


FIGURE 7: Continued.



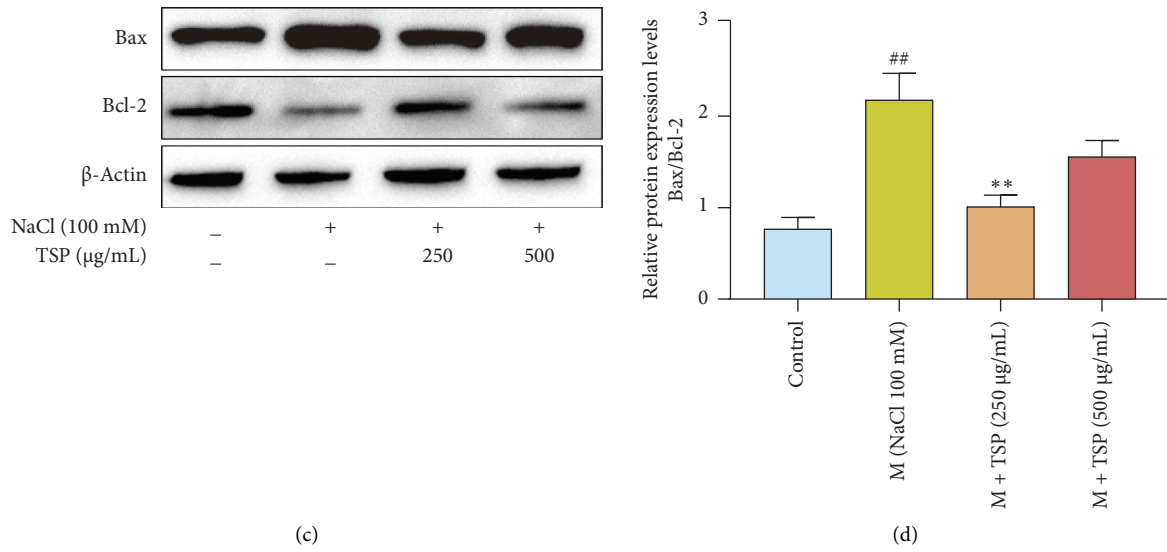


FIGURE 7: Effects of TSP on the cell apoptosis of HCECs induced by NaCl. (a, b) The relative cell apoptosis rate was detected by calcein-AM/PI staining. Calcein-positive cells, green; PI-positive cells, red; and scale bar: 50  $\mu\text{m}$ ; ( $n = 5$ ). (c, d) The protein expression of Bcl-2 and Bax was analyzed by western blot assay. Quantitation of the intensities normalized to  $\beta$ -actin, ( $n = 3$ ). Data are shown as mean  $\pm$  SEM. <sup>##</sup>  $p < 0.01$  vs. control group; and <sup>\*\*</sup>  $p < 0.01$  vs. M group.

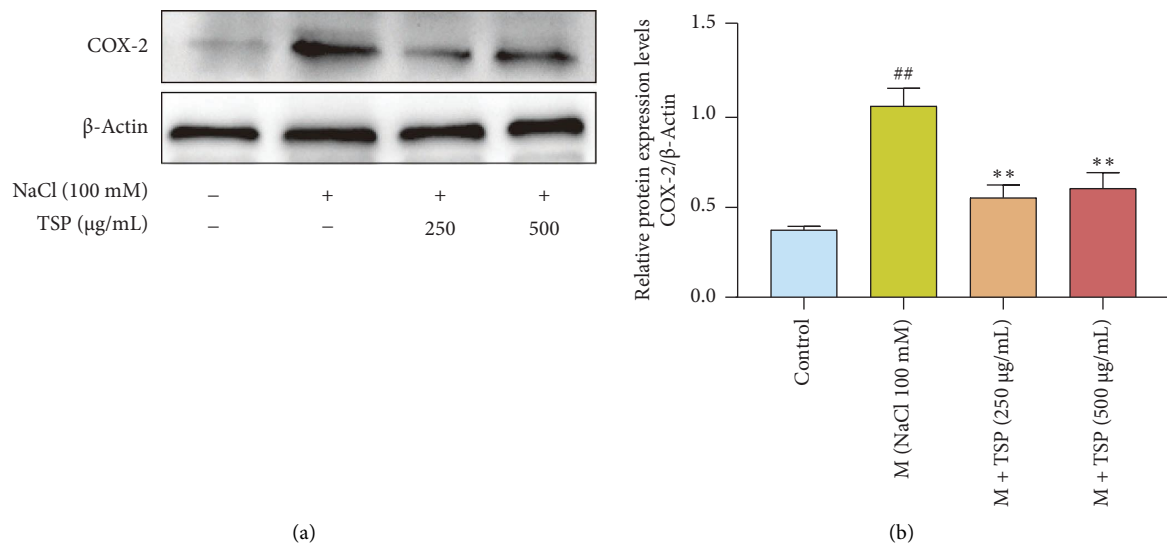


FIGURE 8: Continued.

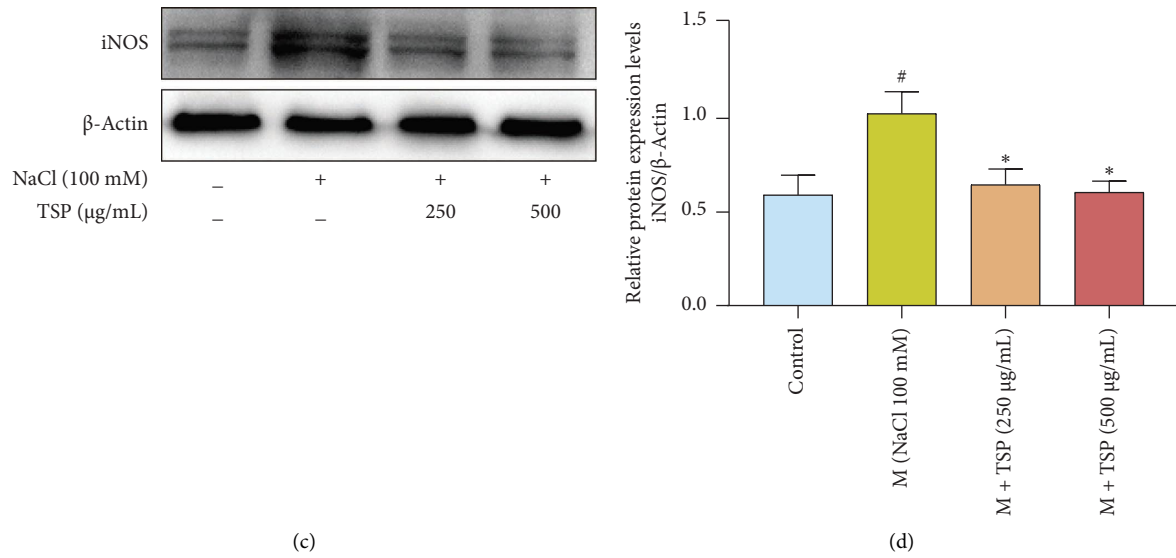


FIGURE 8: Effects of TSP on NaCl-induced inflammation in HCECs. The protein expression of COX-2 and iNOS was analyzed by western blot assay. Quantitation of the intensities normalized to  $\beta$ -actin, ( $n = 3$ ). Data shown as mean  $\pm$  SEM. #  $p < 0.05$ , ##  $p < 0.01$  vs. control group; \*  $p < 0.05$ , \*\*  $p < 0.01$  vs. M group.

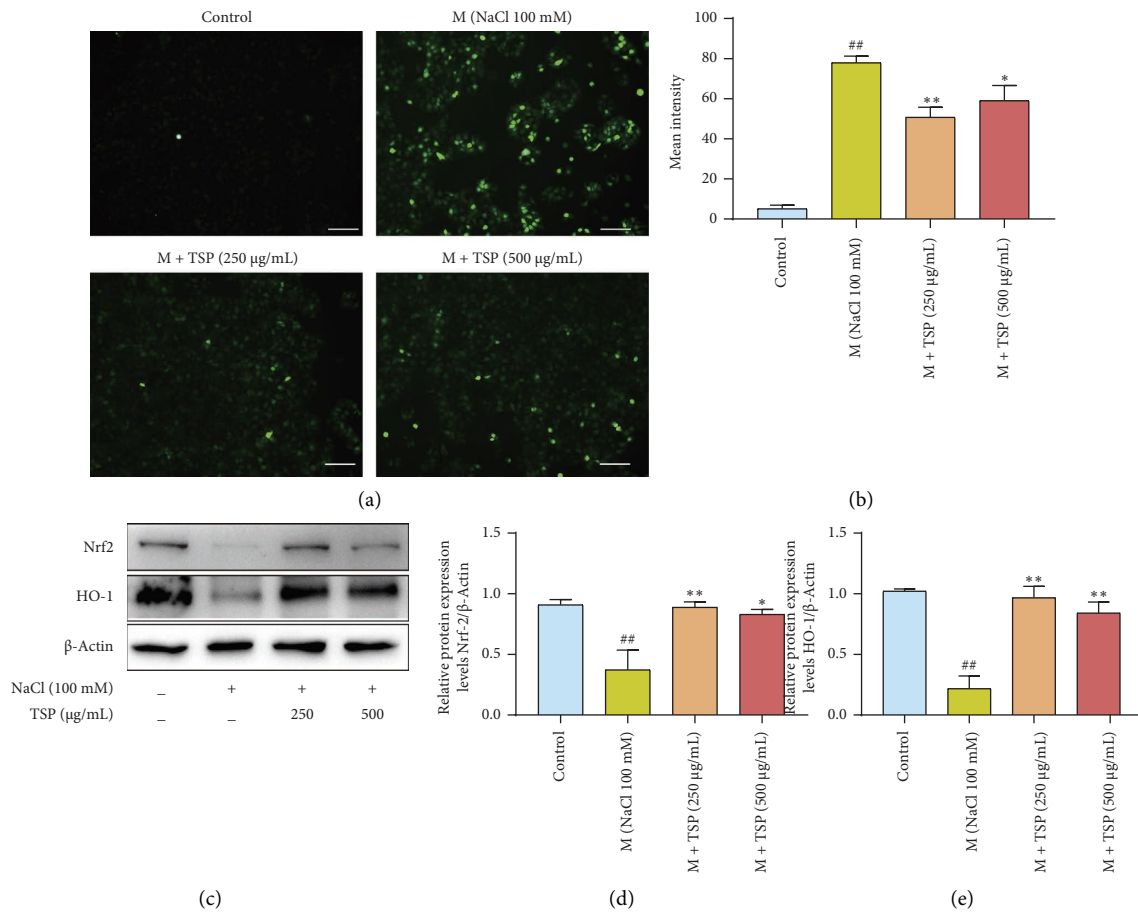


FIGURE 9: Effects of TSP on the ROS/Nrf2/HO-1 axis in HCECs induced by NaCl. (a, b) ROS was detected by DCFH-DA fluorescence staining, and green fluorescence represented ROS; scale bar: 50  $\mu$ m, ( $n = 4$ ). (c–e) The protein expression of Nrf2 and HO-1 was analyzed by western blot assay. Quantitation of the intensities normalized to  $\beta$ -actin ( $n = 3$ ). Data are shown as mean  $\pm$  SEM. ##  $p < 0.01$  vs. control group; \*  $p < 0.05$ , \*\*  $p < 0.01$  vs. M group.

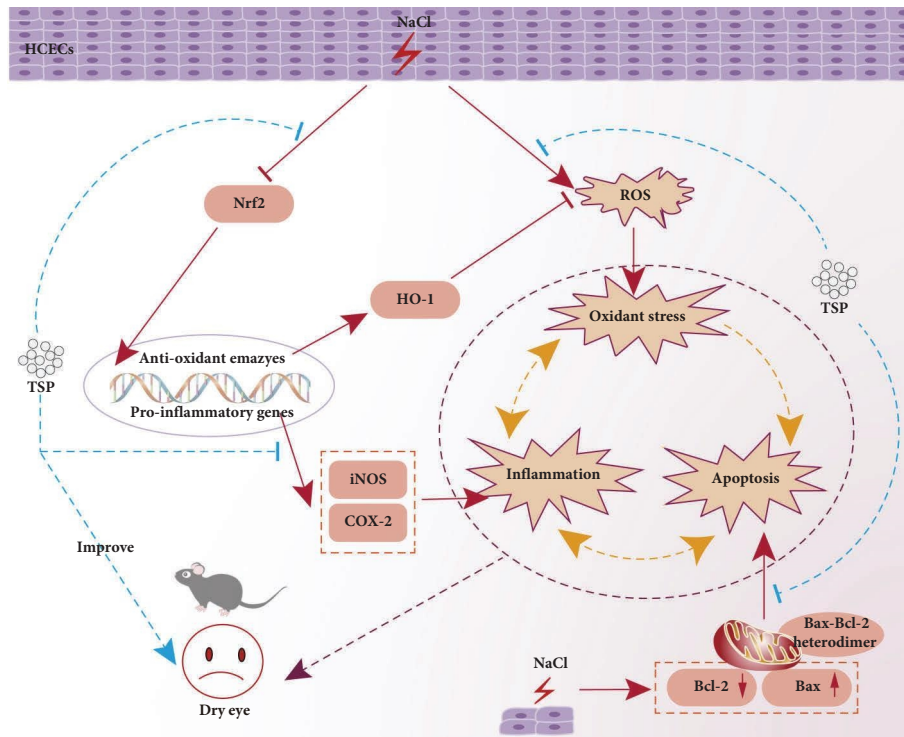


FIGURE 10: Schematic illustration of TSP ameliorates DED by inhibiting apoptosis, inflammation, and oxidative stress. NaCl stimulation blocks Nrf2/HO-1 signalling in HCECs. Impaired Nrf2/HO-1 signal promoted ROS overproduction and triggered COX-2 and iNOS overexpression, resulting in oxidative stress and inflammation. NaCl stimulation also disrupted the balance of Bax/Bcl-2 expression in HCECs, leading to apoptosis. Apoptosis, inflammation, and oxidative stress interact to participate in the pathological process of DED, resulting in mice exhibiting DED symptoms. All these undesirable phenomena were ameliorated by TSP. Collectively, TSP can modulate the pathological process of DED from multiple perspectives, thus improving DED.

decreased tear secretion, increased tear fern score, and decreased corneal epithelial cell layer thickness and the number of GCs in mice. After TSP intervention, these adverse indicators were improved both in HCECs and mice. TSP appears to be comparable to the positive medicine, SH, in improving DED symptoms in DED mice. Here, the potential mechanisms of TSP in ameliorating DED were further investigated in depth through cell and animal models.

Apoptosis plays a critical role in the pathological processes of DED. Numerous studies demonstrate that hyperosmolarity triggers apoptosis in ocular surface cells, especially in corneal epithelial cells [38]. It is well known that a steady tear film is a hallmark of a healthy eye surface. Abnormalities in both tear production and evaporation result in impairment of tear film balance, which is accompanied by variations in tear osmolarity [39]. Tear hyperosmolarity results in corneal epithelial cells apoptosis and causes loss of GCs. Loss of GCs is also associated with apoptosis [40]. Mucin, secreted by CGs, is the component of tears and has a role in maintaining the stability of the tear film and influencing the integrity of the fern-like crystals of the tears [28]. In the present study, mice induced by BAC decreased tear secretion, elevated tear fern score, reduced number of GCs, detached corneal epithelial cells, and affected corneal epithelial cell layer thickness. Those phenomena may be related to apoptosis of ocular surface cells.

Apoptosis is regulated by the relative expression of Bax/Bcl-2. Bcl-2, as an antiapoptotic protein, is instrumental in maintaining mitochondrial function. Overexpression of Bcl-2 inhibits translocation and dimerization of the proapoptotic protein Bax, which exhibits arresting effects on apoptosis [41]. Here, the number of TUNEL-labeled corneal epithelial cells was enhanced in mice exposed to BAC. NaCl stimulation increased the relative apoptosis rate of HCECs and elevated the Bax/Bcl-2 ratio of HCECs. These results are direct evidence for the involvement of apoptosis in DED. After TSP intervention, the indicators of DED were improved in both cell and mice DED models. Thus, TSP may impend the development and progression of DED *via* antiapoptosis. Accordingly, TSP ameliorated DED by exercising antiapoptotic effects.

Inflammation is viewed as a key factor in triggering DED. Corneal epithelial cells are a vital component of the cornea [42]. In normal physiological conditions, corneal epithelial cells contribute substantially to maintaining corneal transparency and preventing the invasion of external pathogens into the eye [43]. Previous studies have established that tear hyperosmolarity can cause inflammation of the ocular surface [44]. Increasing tear osmolarity causes the secretion of proinflammatory factors, chemokines, and matrix metalloproteinases (MMPs), activates mitogen-activated protein kinase, nuclear factor kappa-B, and other signal pathways, and triggers a chain of inflammatory

responses in the ocular surface [45–48]. Many studies indicate that MMPs cleave tight junction proteins, occludin, and zonula occludens-1, which leads to corneal epithelial cells exfoliation [49, 50]. This may be related to the thinning of the corneal epithelial cell layers from our observations in the DED mice. The conjunctiva is an essential element of the ocular surface. It contributes to ensure the ongoing clarity and survival of the ocular cells and stroma. Chronic inflammation leads to conjunctival disorders, one of the important features of which is the loss of CGs [51]. Inflammation exacerbates the loss of CGs, resulting in a deficiency of mucin in tears. Furthermore, tear osmolarity increases with mucin deficiency. Tear hyperpermeability in turn promotes the development of ocular surface inflammation and apoptosis, exacerbating corneal epithelial damage and trapping DED in a vicious cycle [52, 53]. In addition, chronic inflammation results in increased expression of COX-2 and iNOS [54]. In this work, BAC stimulation increased the grade of tear fern-like crystals, diminished corneal epithelial thickness, and promoted the loss of CGs in mice. NaCl excitation upregulated the expression levels of COX-2 and iNOS proteins in HCECs. This evidence suggested that inflammation and DED were connected. After TSP intervention, all these indicators were reversed. TSP contributed to improve tear film stability, repair corneal epithelium, and impend the onset and development of DED possibly associated with its anti-inflammatory effects.

Mounting evidence suggests that oxidative stress orchestrates the pathological process of DED [55]. Overproduction of ROS leads to oxidative stress, which causes lipid oxidation, protein denaturation, and DNA damage, further contributing to inflammation and apoptosis [56]. Oxidative stress is a causal factor in several disorders [57]. In ocular, oxidative stress is associated with most eye diseases, such as glaucoma and cataract. [58]. Remarkably, abnormal ROS production and inflammatory cell infiltration are detected in the ocular tissues of patients with DED [59]. Eyes are susceptible to high levels of ROS because they are directly exposed to UV light, dry, and air pollution for long periods. Additionally, ocular surface oxidative stress induced by hyperosmotic stimulation has been reported [48]. Other research studies demonstrated that excess ROS leads to apoptosis by a mitochondria-dependent pathway [60]. Nrf2/HO-1 is an important pathway for regulating intracellular oxidative stress, inflammation, and apoptosis [61]. Under oxidative stress, Nrf2 enters the nucleus and associates with antioxidant response element [62]. Then, the activities of endogenous antioxidant enzymes (e.g., SOD, HO-1, etc.) were enhanced, and the production of ROS was reduced [62]. Here, the protein expression levels of Nrf2 and HO-1 were significantly reduced, and the level of ROS production was clearly increased after treatment with NaCl for 12 h in HCECs. These results indicate that oxidative stress, together with apoptosis and inflammation, is involved in the onset and development of DED. After TSP intervention, all these unfavourable indicators were improved, which indicated that TSP reversed the onset and development of DED by regulating the ROS/Nrf2/HO-1 axis.

## 5. Conclusions

*In vitro*, TSP restored the cell viability of NaCl-challenged HCECs, reduced relative apoptosis rate and ROS production level, decreased Bax/BcL-2 protein expression rate, down-regulated COX-2 and iNOS protein expression levels, and increased Nrf2 and HO-1 protein expression levels. *In vivo*, TSP increased the length of reddening of cotton threads in BAC-induced DED mice, reduced the grade of its tear ferning, restored the thickness of corneal epithelial cell layer, and inhibited the loss of its GCs and apoptosis of corneal epithelium. In summary, TSP impend the generation and development of DED *via* inhibition of apoptosis, inflammation, and oxidative stress (Figure 10). This study provides a new perspective on the high-value utilization of tilapia skin by-products for processing, and TSP is promising to be developed as a potential product to prevent and manage DED.

## Data Availability

Data are available from the corresponding author upon reasonable request.

## Conflicts of Interest

The authors declare they have no conflicts of interest.

## Authors' Contributions

This study was conceived and designed by Jian Zeng, Chuanyin Hu, and Yun-Tao Zhao. Jian Zeng, Kaishu Deng, Jianyang Du, and Zhiyou Yang performed experiments. Chuanyin Hu, Cuixian Lin, and Shilin Zhang organized and analyzed the data. The original draft was written by Jian Zeng, Chuanyin Hu, and Yun-Tao Zhao. This manuscript was reviewed and edited by Wenjin Wu, Shucheng Liu, Jianyang Du, and Yun-Tao Zhao. All authors have read and approved the published version of the manuscript.

## Acknowledgments

This research was supported by the Special Projects in Key Fields of Colleges and Universities in Guangdong Province (2022ZDZX2026), National Key R&D Program of China (2019YFD0901805), and Special Funds for Scientific and Technological Development of Zhanjiang (2022A01033).

## References

- [1] J. A. Clayton, "Dry eye," *New England Journal of Medicine*, vol. 378, no. 23, pp. 2212–2223, 2018.
- [2] F. Stapleton, M. Alves, V. Y. Bunya et al., "TFOS DEWS II epidemiology report," *Ocular Surface*, vol. 15, no. 3, pp. 334–365, 2017.
- [3] D. A. Sullivan, E. M. Rocha, P. Aragona et al., "TFOS DEWS II sex, gender, and hormones report," *Ocular Surface*, vol. 15, no. 3, pp. 284–333, 2017.
- [4] S. Tellefsen Noland, R. A. Badian, T. P. Utheim et al., "Sex and age differences in symptoms and signs of dry eye disease in

- a Norwegian cohort of patients,” *Ocular Surface*, vol. 19, pp. 68–73, 2021.
- [5] S. Y. Lee, A. Petznick, and L. Tong, “Associations of systemic diseases, smoking and contact lens wear with severity of dry eye,” *Ophthalmic and Physiological Optics*, vol. 32, no. 6, pp. 518–526, 2012.
- [6] M. S. Magno, T. Daniel, M. K. Morthen et al., “The relationship between alcohol consumption and dry eye,” *Ocular Surface*, vol. 21, pp. 87–95, 2021.
- [7] S. Li, K. Ning, J. Zhou et al., “Sleep deprivation disrupts the lacrimal system and induces dry eye disease,” *Experimental and Molecular Medicine*, vol. 50, no. 3, p. e451, 2018.
- [8] J. Li, G. Tan, X. Ding et al., “A mouse dry eye model induced by topical administration of the air pollutant particulate matter 10,” *Biomedicine & Pharmacotherapy*, vol. 96, pp. 524–534, 2017.
- [9] W. S. Kang, E. Jung, and J. Kim, “Aucuba japonica extract and aucubin prevent desiccating stress-induced corneal epithelial cell injury and improve tear secretion in a mouse model of dry eye disease,” *Molecules*, vol. 23, no. 10, p. 2599, 2018.
- [10] Q. He, Z. Chen, C. Xie, L. Liu, H. Yang, and R. Wei, “Relationship between dry eye disease and emotional disorder: the mediating effect of health anxiety,” *Frontiers in Public Health*, vol. 10, Article ID 771554, 2022.
- [11] C.-Y. Tsai, Z. L. Jiesisibieke, and T.-H. Tung, “Association between dry eye disease and depression: an umbrella review,” *Frontiers in Public Health*, vol. 10, Article ID 910608, 2022.
- [12] M. Labetoulle, J. M. Benitez-Del-Castillo, S. Barabino et al., “Artificial tears: biological role of their ingredients in the management of dry eye disease,” *International Journal of Molecular Sciences*, vol. 23, no. 5, p. 2434, 2022.
- [13] B. Park, I. S. Lee, S. W. Hyun et al., “The protective effect of polygonum cuspidatum (PCE) aqueous extract in a dry eye model,” *Nutrients*, vol. 10, p. 1550, 2018.
- [14] C. E. Kim, H. N. Oh, J. H. Lee, and J. W. Yang, “Effects of chondrocyte-derived extracellular matrix in a dry eye mouse model,” *Molecular Vision*, vol. 21, pp. 1210–1223, 2015.
- [15] W. Y. Mo, Y. B. Man, and M. H. Wong, “Use of food waste, fish waste and food processing waste for China’s aquaculture industry: needs and challenge,” *Science of the Total Environment*, vol. 613–614, pp. 635–643, 2018.
- [16] L. Sun, H. Hou, B. Li, and Y. Zhang, “Characterization of acid- and pepsin-soluble collagen extracted from the skin of Nile tilapia (*Oreochromis niloticus*),” *International Journal of Biological Macromolecules*, vol. 99, pp. 8–14, 2017.
- [17] H. S. H. Munawaroh, G. G. Gumilar, J. D. Berliana et al., “In silico proteolysis and molecular interaction of tilapia (*Oreochromis niloticus*) skin collagen-derived peptides for environmental remediation,” *Environmental Research*, vol. 212, Article ID 113002, 2022.
- [18] M. Valero-Vello, C. Peris-Martinez, J. J. Garcia-Medina et al., “Searching for the antioxidant, anti-inflammatory, and neuroprotective potential of natural food and nutritional supplements for ocular health in the mediterranean population,” *Foods*, vol. 10, no. 6, p. 1231, 2021.
- [19] D. D. Li, W. J. Li, S. Z. Kong et al., “Protective effects of collagen polypeptide from tilapia skin against injuries to the liver and kidneys of mice induced by d-galactose,” *Biomedicine & Pharmacotherapy*, vol. 117, Article ID 109204, 2019.
- [20] F. Mei, J. Liu, J. Wu et al., “Collagen peptides isolated from *Salmo salar* and *Tilapia nilotica* skin accelerate wound healing by altering cutaneous microbiome colonization via upregulated NOD2 and BD14,” *Journal of Agricultural and Food Chemistry*, vol. 68, no. 6, pp. 1621–1633, 2020.
- [21] Y. Y. Ma, D. D. Zhang, M. Q. Liu et al., “Identification of antioxidant peptides derived from *Tilapia (Oreochromis niloticus)* skin and their mechanism of action by molecular docking,” *Foods*, vol. 11, no. 17, p. 2576, 2022.
- [22] T. S. Vo, D. H. Ngo, J. A. Kim, B. Ryu, and S. K. Kim, “An antihypertensive peptide from tilapia gelatin diminishes free radical formation in murine microglial cells,” *Journal of Agricultural and Food Chemistry*, vol. 59, no. 22, Article ID 12193, 2011.
- [23] Y. T. Zhao, H. Yin, C. Hu et al., “Tilapia skin peptides ameliorate cyclophosphamide-induced anxiety- and depression-like behavior via improving oxidative stress, neuroinflammation, neuron apoptosis, and neurogenesis in mice,” *Frontiers in Nutrition*, vol. 9, Article ID 882175, 2022.
- [24] H. C. Lin, A. M. Alashi, R. E. Aluko, B. Sun Pan, and Y. W. Chang, “Antihypertensive properties of tilapia (*Oreochromis spp.*) frame and skin enzymatic protein hydrolysates,” *Food & Nutrition Research*, vol. 61, no. 1, Article ID 1391666, 2017.
- [25] Y. T. Zhao, H. Yin, C. Hu et al., “Tilapia skin peptides restore cyclophosphamide-induced premature ovarian failure via inhibiting oxidative stress and apoptosis in mice,” *Food & Function*, vol. 13, no. 3, pp. 1668–1679, 2022.
- [26] Z. Lin, Y. Zhou, Y. Wang et al., “Serine protease inhibitor A3K suppressed the formation of ocular surface squamous metaplasia in a mouse model of experimental dry eye,” *Investigative Ophthalmology & Visual Science*, vol. 55, no. 9, pp. 5813–5820, 2014.
- [27] M. Yamaga, T. Imada, H. Tani, S. Nakamura, A. Yamaki, and K. Tsubota, “Acetylcholine and royal jelly fatty acid combinations as potential dry eye treatment components in mice,” *Nutrients*, vol. 13, no. 8, p. 2536, 2021.
- [28] Y. J. Tang, H. H. Chang, C. Y. Tsai, L. Y. Chen, and D. P. Lin, “Establishment of a tear ferning test protocol in the mouse model,” *Translational Vision Science & Technology*, vol. 9, no. 13, p. 1, 2020.
- [29] Y. Yang, C. Huang, X. Lin et al., “0.005% preservative-free latanoprost induces dry eye-like ocular surface damage via promotion of inflammation in mice,” *Investigative Ophthalmology & Visual Science*, vol. 59, no. 8, pp. 3375–3384, 2018.
- [30] B. Ma, L. Pang, P. Huang et al., “Topical delivery of levocarnitine to the cornea and anterior eye by thermosensitive in-situ gel for dry eye disease,” *Drug Design, Development and Therapy*, vol. 15, pp. 2357–2373, 2021.
- [31] J. Wen, J. Doerner, S. Chalmers et al., “B cell and/or auto-antibody deficiency do not prevent neuropsychiatric disease in murine systemic lupus erythematosus,” *Journal of Neuroinflammation*, vol. 13, no. 1, p. 73, 2016.
- [32] Y. Jin, X. Tang, X. Cao et al., “4-((5-(Tert-butyl)-3-chloro-2-hydroxybenzyl) amino)-2-hydroxybenzoic acid protects against oxygen-glucose deprivation/reperfusion injury,” *Life Sciences*, vol. 204, pp. 46–54, 2018.
- [33] Q. Jiang, D. Y. Su, Z. Z. Wang et al., “Retina as a window to cerebral dysfunction following studies with circRNA signature during neurodegeneration,” *Theranostics*, vol. 11, no. 4, pp. 1814–1827, 2021.
- [34] Q. Miao, Y. Xu, H. Zhang, P. Xu, and J. Ye, “Cigarette smoke induces ROS mediated autophagy impairment in human corneal epithelial cells,” *Environmental Pollution*, vol. 245, pp. 389–397, 2019.
- [35] Y. T. Zhao, L. Zhang, H. Yin et al., “Hydroxytyrosol alleviates oxidative stress and neuroinflammation and enhances

- hippocampal neurotrophic signaling to improve stress-induced depressive behaviors in mice,” *Food & Function*, vol. 12, pp. 5478–5487, 2021.
- [36] L. E. Downie, S. M. Ng, K. B. Lindsley, E. K. Akpek, K. B. Lindsley, and E. K. Akpek, “Omega-3 and omega-6 polyunsaturated fatty acids for dry eye disease,” *Cochrane Database of Systematic Reviews*, vol. 12, Article ID CD011016, 2019.
- [37] L. E. Downie and S. M. Ng, “The pathophysiology of dry eye disease: what we know and future directions for research,” *Cochrane Database of Systematic Reviews*, vol. 124, pp. S4–S13, 2017.
- [38] N. Lyu, J. Zhang, Y. Dai, J. Xiang, Y. Li, and J. Xu, “Calcitriol inhibits apoptosis via activation of autophagy in hyperosmotic stress stimulated corneal epithelial cells *In vivo* and *In vitro*,” *Experimental Eye Research*, vol. 200, Article ID 108210, 2020.
- [39] P. E. King-Smith, K. S. Reuter, R. J. Braun, J. J. Nichols, and K. K. Nichols, “Tear film breakup and structure studied by simultaneous video recording of fluorescence and tear film lipid layer images,” *Investigative Ophthalmology & Visual Science*, vol. 54, no. 7, pp. 4900–4909, 2013.
- [40] T. Yamaguchi, “Inflammatory response in dry eye,” *Investigative Ophthalmology & Visual Science*, vol. 59, no. 14, Article ID DES192, 2018.
- [41] M. Raisova, A. M. Hossini, J. Eberle et al., “The Bax/Bcl-2 ratio determines the susceptibility of human melanoma cells to CD95/Fas-mediated apoptosis,” *Journal of Investigative Dermatology*, vol. 117, no. 2, pp. 333–340, 2001.
- [42] M. Eslani, A. Movahedan, N. Afsharkhamseh, H. Sroussi, and A. R. Djalilian, “The role of toll-like receptor 4 in corneal epithelial wound healing,” *Investigative Ophthalmology & Visual Science*, vol. 55, no. 9, pp. 6108–6115, 2014.
- [43] S. Kolli, S. Bojic, A. E. Ghareeb, M. Kurzawa-Akanbi, F. C. Figueiredo, and M. Lako, “The role of nerve growth factor in maintaining proliferative capacity, colony-forming efficiency, and the limbal stem cell phenotype,” *Stem Cells*, vol. 37, no. 1, pp. 139–149, 2019.
- [44] Q. Zheng, Y. Ren, P. S. Reinach et al., “Reactive oxygen species activated NLRP3 inflammasomes initiate inflammation in hyperosmolarity stressed human corneal epithelial cells and environment-induced dry eye patients,” *Experimental Eye Research*, vol. 134, pp. 133–140, 2015.
- [45] C. Baudouin, P. Aragona, E. M. Messmer et al., “Role of hyperosmolarity in the pathogenesis and management of dry eye disease: proceedings of the OCEAN group meeting,” *Ocular Surface*, vol. 11, no. 4, pp. 246–258, 2013.
- [46] R. Deng, Z. Su, X. Hua, Z. Zhang, D. Q. Li, and S. C. Pflugfelder, “Osmoprotectants suppress the production and activity of matrix metalloproteinases induced by hyperosmolarity in primary human corneal epithelial cells,” *Molecular Vision*, vol. 20, pp. 1243–1252, 2014.
- [47] C. Wang, X. Shi, X. Chen et al., “17-beta-estradiol inhibits hyperosmolarity-induced proinflammatory cytokine elevation via the p38 MAPK pathway in human corneal epithelial cells,” *Molecular Vision*, vol. 18, pp. 1115–1122, 2012.
- [48] B. Park, K. Jo, T. G. Lee, S. W. Hyun, J. S. Kim, and C. S. Kim, “Polydatin inhibits NLRP3 inflammasome in dry eye disease by attenuating oxidative stress and inhibiting the NF- $\kappa$ B pathway,” *Nutrients*, vol. 11, p. 2792, 2019.
- [49] E. C. Jamerson, A. M. Elhusseiny, R. H. ElSheikh, T. K. Eleiwa, and Y. M. El Sayed, “Role of matrix metalloproteinase 9 in ocular surface disorders,” *Eye and Contact Lens: Science and Clinical Practice*, vol. 46, no. 2, pp. S57–S63, 2020.
- [50] C. S. De Paiva, R. M. Corrales, A. L. Villarreal et al., “Corticosteroid and doxycycline suppress MMP-9 and inflammatory cytokine expression, MAPK activation in the corneal epithelium in experimental dry eye,” *Experimental Eye Research*, vol. 83, no. 3, pp. 526–535, 2006.
- [51] F. S. Usuba, C. G. S. Saad, N. E. Aikawa et al., “Improvement of conjunctival cytological grade and tear production in Ankylosing Spondylitis patients under TNF inhibitors: a long-term follow-up,” *Scientific Reports*, vol. 10, no. 1, p. 334, 2020.
- [52] K. S. Khimani, J. A. Go, R. G. De Souza et al., “Regional comparison of goblet cell number and area in exposed and covered dry eyes and their correlation with tear MUC5AC,” *Scientific Reports*, vol. 10, no. 1, p. 2933, 2020.
- [53] S. Tibrewal, Y. Ivanir, J. Sarkar et al., “Hyperosmolar stress induces neutrophil extracellular trap formation: implications for dry eye disease,” *Investigative Ophthalmology & Visual Science*, vol. 55, no. 12, pp. 7961–7969, 2014.
- [54] H. Lim, J. R. Noh, Y. H. Kim et al., “Anti-atherogenic effect of Humulus japonicus in apolipoprotein E-deficient mice,” *International Journal of Molecular Medicine*, vol. 38, no. 4, pp. 1101–1110, 2016.
- [55] V. Navel, V. Sapin, F. Henrioux et al., “Oxidative and anti-oxidative stress markers in dry eye disease: a systematic review and meta-analysis,” *Acta Ophthalmologica*, vol. 100, no. 1, pp. 45–57, 2022.
- [56] X. Zhao, X. Tao, L. Xu et al., “Dioscin induces apoptosis in human cervical carcinoma HeLa and SiHa cells through ROS-mediated DNA damage and the mitochondrial signaling pathway,” *Molecules*, vol. 21, no. 6, p. 730, 2016.
- [57] M. Dogru, T. Kojima, C. Simsek, and K. Tsubota, “Potential role of oxidative stress in ocular surface inflammation and dry eye disease,” *Investigative Ophthalmology & Visual Science*, vol. 59, no. 14, Article ID DES163, 2018.
- [58] M. Vivero-Lopez, A. Muras, D. Silva et al., “Resveratrol-loaded hydrogel contact lenses with antioxidant and anti-biofilm performance,” *Pharmaceutics*, vol. 13, no. 4, p. 532, 2021.
- [59] Y. Li, H. Liu, W. Zeng, and J. Wei, “Edaravone protects against hyperosmolarity-induced oxidative stress and apoptosis in primary human corneal epithelial cells,” *PLoS One*, vol. 12, no. 3, Article ID e0174437, 2017.
- [60] X. Chen, X. Dai, P. Zou et al., “Curcuminoid EF24 enhances the anti-tumour activity of Akt inhibitor MK-2206 through ROS-mediated endoplasmic reticulum stress and mitochondrial dysfunction in gastric cancer,” *British Journal of Pharmacology*, vol. 174, no. 10, pp. 1131–1146, 2017.
- [61] H. Mylroie, O. Dumont, A. Bauer et al., “PKC $\epsilon$ -CREB-Nrf2 signalling induces HO-1 in the vascular endothelium and enhances resistance to inflammation and apoptosis,” *Cardiovascular Research*, vol. 106, no. 3, pp. 509–519, 2015.
- [62] Y. Wang, X. Chen, Z. Huang et al., “Dietary ferulic acid supplementation improves antioxidant capacity and lipid metabolism in weaned piglets,” *Nutrients*, vol. 12, p. 3811, 2020.